MicroRNA-500a-5p inhibits colorectal cancer cell invasion and epithelial-mesenchymal transition

WEIMEI TANG[1], LINJIE HONG[1], WEIYU DAI[1], JIAYING LI[1], HUIQIONG ZHU[1], JIANJIAO LIN[2], QIONG YANG[3], YUSI WANG[1], ZHIZHAO LIN[1], MENGWEI LIU[1], YIZHI XIAO[1], YI ZHANG[1], XIAOSHENG WU[1], JING WANG[1], YAYING CHEN[4], HONGSONG HU[2], SIDE LIU[1], JIDE WANG[1,2] and LI XIANG[2]

[1]Guangdong Provincial Key Laboratory of Gastroenterology, Department of Gastroenterology, Nanfang Hospital, Southern Medical University, Guangzhou, Guangdong 510515; [2]Department of Gastroenterology, Longgang District People's Hospital, Shenzhen, Guangdong 518172; [3]Department of Gastroenterology, The Second Affiliated Hospital University of South China, Hengyang, Hunan 421001; [4]Department of Gastroenterology, The Third Affiliated Hospital of Guangzhou Medical University, Guangzhou, Guangdong 510150, P.R. China

Received July 4, 2019; Accepted January 30, 2020

DOI: 10.3892/ijo.2020.5015

Abstract. The development of malignant tumors is a series of complex processes, the majority of which have not been elucidated. The aim of the present study was to investigate the microRNAs (miRNAs/miR) that affect the migration and invasion abilities of CRC cells. Our previous reports have revealed that miR-500a-5p suppressed CRC cell growth and malignant transformation. The present study demonstrated that overexpression of miR-500a-5p reduced the expression of vimentin, while increasing the expression of E-cadherin. Inhibition of miR-500a-5p resulted in spindle-like morphological changes and reorganization of F-actin in CRC cells. Furthermore, miR-500a-5p attenuated the transforming growth factor-β signaling pathway in EMT. Additionally, emodin inhibited the miR-500a-5p inhibitor and suppressed the EMT process. In animal models of metastasis using nude mice, EMT and LoVo cell metastasis was modulated by miR-500a-5p. Therefore, the findings of the present study demonstrated that miR-500a-5p is associated with a positive therapeutic outcome in terms of invasion/migration of CRC cells and mesenchymal-like cell changes.

Correspondence to: Dr Li Xiang, Department of Gastroenterology, Longgang District People's Hospital, 53 Aixin Road, Shenzhen, Guangdong 518172, P.R. China
E-mail: shellyxiang@sina.com

Professor Jide Wang, Guangdong Provincial Key Laboratory of Gastroenterology, Department of Gastroenterology, Nanfang Hospital, Southern Medical University, 1838 Guangzhou Avenue North, Guangzhou, Guangdong 510515, P.R. China
E-mail: jidewang55@163.com

Abbreviations: EMT, epithelial-mesenchymal transition; CRC, colorectal cancer; TGF-β1, recombinant human transforming growth factor β-1

Key words: miR-500a-5p, epithelial-mesenchymal transition, transforming growth factor-β1, colorectal cancer, emodin

Introduction

CRC has a high mortality rate in China (1,2), accounting for >600,000 deaths annually, despite the advances in treatment. The high CRC mortality rates are due to the high frequency of tumor recurrence following surgical resection (3,4). Hence, it is important to investigate the molecular and cellular growth processes of CRC in order to identify potential treatment targets.

MicroRNAs (miRNAs/miRs) are aberrantly expressed in numerous types of cancers and can function either as tumor suppressors or oncogenes. For example, Zhang *et al* (5) found miR-187 was downregulated in colorectal cancer, while Zhang *et al* (6) verified miR-646 was downregulated in gastric cancer (GC) tissues and Liu *et al* (7) found that miR-935 was upregulated in liver cancer tissues and cells. miRNAs are a single-stranded class of RNAs that cause inhibition of gene expression at the post-transcriptional level by instantly binding to the 3'-untranslated regions (3'UTRs) of mRNAs. This inhibits their translation process and causes degradation. miR-500a is located within the p11 locus on the X chromosome and has two arms: miR-500a-5p and miR-500a-3p. hsa-miR-500a-5p and hsa-miR-500a-3p were previously referred to as hsa-miR-500a and hsa-miR-500a*, respectively (http://mirdb.org/cgi-bin/search.cgi). miR-500a-5p was previously reported to be an important factor in the development of cancer. The expression of miR-500a-5p was found to be markedly upregulated in human hepatocellular carcinoma (8), chronic lymphocytic leukemia (9), breast cancer (10) and lung cancer (11), while it was found to be downregulated in CRC (12), indicating miR-500a-5p has a role in tumorigenesis. However, the role of miR-500a-5p has not been fully elucidated in CRC.

EMT is a key step in tumor metastasis (13,14). EMT represents the loss of cell polarity and cell-cell adhesion

by epithelial cells, which results in transformation to a mesenchymal phenotype, as well as migration and invasion, providing a mechanism for cancer development (15,16). Keratin and vimentin filaments regulate the intermediate filament composition, while downregulation of E-cadherin reinforces the destabilization of adhesion junctions and MMP9 enhances extracellular matrix protein degradation and enables invasion (17). Repression of epithelial markers (cytokeratins and E-cadherin) and induction of mesenchymal markers vimentin and matrix metallopeptidase (MMP)-9, constitute an essential part of the EMT process. EMT is physiologically initiated by certain autocrine factors, with TGF-β being the strongest inducer that functions in the majority of epithelial cell types tested *in vivo* (18). Various studies have revealed that miRNAs affect the regulation of EMT during cancer progression and metastasis (5,6,19). For example, tumor suppressor miR-1271 binds to a particular target mRNA in EMT-related genes, ZEB1 and TWIST1, and increased expression of miR-1271 is considered to be an adverse prognostic indicator in pancreatic cancer (19). Furthermore, miR-500a-5p has been found to act as a tumor suppressor in CRC (12). However, the mechanism underlying the tumor suppressor miR-500a-5p during EMT in CRC remains unclear.

The Rhubarb plant roots (*Rheum palmatum* L.), which are used as laxatives in Traditional Chinese Medicine, contain rhein, aloe-emodin, and emodin (20-22). Emodin is known for its antibacterial, anti-inflammatory and immunosuppressive properties (23). The anticancer properties of emodin have been investigated primarily in lung (24), liver (25) and stomach cancer (26), as well as CRC (27). It was previously demonstrated that emodin can downregulate the expression of the mesenchymal marker, vimentin, and upregulate the expression of epithelial markers, such as E-cadherin, in gastric and pancreatic cancer cells by increasing the content of miRNA (28,29). However, the mechanism by which emodin regulates miR-500a-5p expression through EMT-like processes in CRC cells has not been investigated.

The aim of the present study was to investigate whether transfecting CRC cells with miR-500a-5p inhibitors would result in EMT phenotypes, and to determine the role of transforming growth factor (TGF)-β in the invasion of tumor cells, as well as the effect of miR-500a-5p on TGF-β1-induced EMT. In addition, the effect of emodin on miR-500a-5p inhibitor-induced EMT in CRC cells was also investigated.

Materials and methods

Reagents and cell culture. The human SW1116 (Dukes' type A, grade III), SW480 (Dukes' type B) and LoVo (Dukes' type C, grade IV) CRC cell lines were purchased from American Type Culture Collection (30). The cells were cultured using RPMI-1640 medium (Thermo Fisher Scientific, Inc.) and supplemented with 10% fetal bovine serum (FBS, Gibco; Thermo Fisher Scientific, Inc.), 100 mg/ml streptomycin and 100 mg/ml penicillin at 37˚C in a humidified incubator with 5% CO_2.

Recombinant human TGF-β1 (cat. no. 240-B) was purchased from R&D Systems, Inc. Emodin was purchased from Sigma-Aldrich (Merck KGaA). Rabbit polyclonal anti-E-cadherin [cat. no. 20874-1-AP; western blot analysis: 1:5,000 dilution; immunohistochemistry (IHC), 1:1,000 dilution; immunofluorescence, 1:100 dilution] and mouse monoclonal anti-vimentin (cat. no. 60330-1-Ig; western blot analysis: 1:5,000 dilution; IHC, 1:2,000 dilution; immunofluorescence, 1:100 dilution) antibodies were purchased from ProteinTech Group, Inc. Mouse monoclonal anti-GAPDH antibody (cat. no. RM2002; western blot analysis: 1:5,000 dilution) was purchased from Beijing Ray Antibody Biotech. Secondary antibodies, including Alexa Fluor 594 (red)-conjugated goat anti-rabbit IgG (cat. no. ZF-0516) and Alexa Fluor 488 (green)-conjugated goat anti-mouse IgG antibodies (cat. no. ZF-0512) were purchased from OriGene Technologies, Inc.

Oligonucleotide transfection. miR-500a-5p mimics, miR-500a-5p mimics control (m-NC), miR-500a-5p inhibitor and miR-500a-5p inhibitor control (i-NC) were all purchased from Shanghai GenePharma Co., Ltd.. For miRNA transfections, cells were seeded at a density of $5x10^4$ cells/ml into 24-well plates 1-2 days prior to transfection until the confluency reached 50-60%. miR-500a-5p mimics (40 nM), miR-500a-5p inhibitor (100 nM) or their corresponding controls miR (m-NC, 40 nM and i-NC, 100 nM) were transfected into CRC cells using Lipofectamine® 3000 reagent for 36 h (Invitrogen; Thermo Fisher Scientific, Inc.) according to the manufacturer's instructions. Following which, transfection efficacy was determined using reverse transcription-quantitative PCR (RT-qPCR). When m-NC or mimics were combined with treatment of TGF-β1, the CRC cells were transfected with miR-500a-5p mimics or m-NC for 24 h, then treated with 5 ng/ml TGF-β1 for 24 h. When i-NC or miR-500a-5p inhibitor were combined with treatment of emodin, 80 μM Emodin was used for 48 h following transfection with i-NC or miR-500a-5p inhibitor for 24 h.

Treatment with TGF-β1. Recombinant human TGF-β1 (cat. no. 240-B) was purchased from R&D Systems, Inc. The SW1116 and LoVo cells were transfected with miR-500a-5p or m-NC for 24 h, and then treated with 0, 1, 3, 5 ng/ml TGF-β1 for 48 h or 5 ng/ml TGF-β1 for 0, 12, 24 and 48 h. The expression of miR-500a-5p was subsequently detected using qPCR.

Western blot analysis and protein extraction. Protein was extracted from cells that reached 80-90% confluency during the exponential growth phase and protein expression was detected using western blot analysis. For emodin treatment, cells were seeded in the 6-well plate and different concentrations (0, 20, 40, 60, 80 μM) of emodin were added to the medium until the cell density reached 80% for 48 h. Cells were digested on the ice with RIPA lysis buffer (cat. no. P0013K; Beyotime Institute of Biotechnology), including a protease inhibitor. Protein were separated using 10% SDS-PAGE and proteins were transferred onto Immobilon-P membranes (EMD Millipore; Merck KGaA). After blocking with 5% skimmed milk in PBS-Tween-20 at room temperature for 1 h, the membranes were incubated with aforementioned primary antibodies overnight at 4˚C. Subsequently, a horseradish peroxidase (HRP)-conjugated goat anti-rabbit IgG (cat. no. ZB-2301) or goat anti-mouse IgG (cat. no. ZB-2305) secondary antibodies (dilution 1:10,000; both OriGene Technologies, Inc.) was used

at room temperature for 1 h. The proteins were visualised using ECL (PerkinElmer, Inc.).

RT-qPCR. Total RNA was extracted from cells using TRIzol® reagent (Invitrogen; Thermo Fisher Scientific, Inc.) according to the manufacturer's protocol and quantified with a Nanodrop 2000 (Thermo Fisher Scientific, Inc.). RT was performed using the Thermoscript RT System (Invitrogen; Thermo Fisher Scientific, Inc.). The sequences of the primer used were as follows: E-cadherin forward, 5'-TGCCCAGAAAAT GAAAAAGG-3' and reverse, 5'-GTGTATGTGGCAATGCG TTC-3'; vimentin forward, 5'-GGAGCTACGTGACTACGT CCA-3' and reverse, 5'-CTTGAACTCGGTGTTGATGG-3'; GAPDH (used as internal control) forward, 5'-GTCAACGGA TTTGGTCGTATTG-3' and reverse, 5'-CTCCTGGAAGAT GGTGATGGG-3'.

For miR-500a-5p expression analysis, miRNA reverse transcription reaction was performed using All-in-One™ miRNA First-Strand cDNA Synthesis kit (cat. no. AMRT-0020;) and qPCR was performed using All-in-One™ miRNA RT-qPCR Detection kit (cat. no. AOMD-Q020; both GeneCopoeia, Inc.). The miR-500a-5p primer (cat. no. HmiRQP0545) and U6 primer (cat. no. HmiRQP9001) were purchased from GeneCopoeia, Inc.. The thermocycling conditions for qPCR was set as pre-denaturation at 95˚C for 10 min, and 40 cycles of denaturation at 95˚C for 10 sec, annealing at 60˚C for 20 sec, and extension at 72˚C for 20 seconds. The small nuclear RNA U6 was used as the internal reference. The relative expression was calculated using the $2^{-\Delta\Delta Cq}$ method (31).

Immunofluorescence. SW1116 or LoVo cells were cultured at a density of $1x10^5$ cells/ml on coverslips and cultured at normal culture conditions (as aforementioned) until the cells reached 30-40% confluency and then were fixed with 4% paraformaldehyde at room temperature for 30 min. Then permeated with 0.2% Triton X-100 for 5 min. Non-specific binding was blocked using 1% bovine serum albumin (Sigma-Aldrich; Merck KGaA). The cells were incubated with aforementioned primary antibodies against E-cadherin and vimentin. Following washing with PBS, the cells were incubated with Alexa Fluor 594 (red)-conjugated goat anti-rabbit IgG and Alexa Fluor 488 (green)-conjugated goat anti-mouse IgG antibodies with dilution of 1:100. Cell nuclei were stained with 1 μg/ml Hoechst 33258 at room temperature for 30 min. The coverslips were then examined using an Olympus CKX 41 fluorescence microscope (Olympus Corporation) at x400 magnification.

F-actin cytoskeleton staining. The cells were cultured at a density of $1x10^5$ cells/ml with 10% FBS at 37˚C and 5% CO_2 on coverslips in a 24-well chamber until the cells reached 30-40% confluency. PBS was used to wash the cells, following which they were fixed in 4% paraformaldehyde at room temperature for 30 min. Following treatment with 0.2% Triton X-100, the cells were incubated with 5 U/ml phalloidin-FITC (Molecular Probes; Thermo Fisher Scientific, Inc.) in PBS for 1 h at a 1:40 dilution. The nuclei were stained with 1 μg/ml Hoechst 33258 at room temperature for 30 min. F-actin cytoskeleton staining was evaluated using a fluorescence microscope at x400 magnification.

Cell invasion analysis. Transwell chambers (BD Biosciences) were used to analyse the invasion ability of CRC cells. The LoVo or SW1116 cells were transfected with miR-500a-5p mimics or inhibitor and suspended in serum-free RPMI-1640 medium. A total of 200 μl RPMI-1640 medium ($1x10^5$ cells/ml) were placed into the upper chamber of Matrigel-coated (at 37˚C for 2 h) Transwell chambers (BD Biosciences) with a PC membrane with a pore size of 8.0 μm. RPMI-1640 (500 μl) supplemented with 20% FBS was placed in the bottom chamber. After 1 complete day, residual cells on the upper surface of the membrane were carefully detached with a cotton swab. The cells that had migrated to the lower surface of the membrane were fixed with methanol for 15 min at room temperature and visualized by staining with 0.1% crystal violet solution at room temperature for 30 min. Images of the invading cells were obtained and were quantified using Axiovert 200 inverted microscope (Carl Zeiss AG) at a magnification of x200, in at least five random fields per filter. Each experiment was repeated independently, three times.

Lentiviral vector construction and transduction. The lentiviral vector was transducted and used for subsequent experimentation after two weeks of puromycin (2 μg/ml) resistance screening. The miR-500a-5p lentivirus was constructed by Shanghai GeneChem Co., Ltd. The red fluorescent protein (RFP) and puromycin resistance genes (Shanghai GeneChem Co., Ltd.) were cloned into a miR-500a-5p lentiviral expression vector (Ubi-MCS-SV40-Cherry) and then transduced into the lentiviral packaging cell line 293T. Polybrene (Shanghai GeneChem Co., Ltd.) was added to the CRC cell lines to a final concentration of 5 μg/ml for stable transduction. Screening for drug resistance with puromycin was performed for 2 weeks to construct stable expression cells. Fluorescence was observed under a fluorescence microscope at x100 magnification and the efficiency was verified using qPCR.

Animal models. A total of 6 BALB/c-nu/nu female mice, (4-6 weeks old; weight 16-20 g), were purchased from the Laboratory Animal Unit, Southern Medical University. Mice were housed three per cage in a specific-pathogen free laboratory and maintained with food and water *ad libitum* at a constant ambient temperature with 12-h light/dark cycle. To evaluate the miR-500a-5p *in vivo* effects on the metastatic ability of CRC cells, nude mice were randomly divided into two groups (m-NC-RFP and miR-500a-5p-RFP group; n=3 per group). Subsequently, $5x10^6$ m-NC-RFP/LoVo or miR-500a-5p-RFP/LoVo cells that were transducted with lentivirus, as aforementioned, (50 μl) were administered by slow injection into the spleen via a 25-gauge needle. After 4 weeks, the mice were euthanized and their livers were removed. *In Vivo* F Imaging System (Kodak) was used to evaluate the fluorescence and number of tumor metastasis. Liver metastatic tissues (4-μm) were fixed in 10% formalin for 24 h, paraffin-embedded at room temperature (Wuhan Servicebio Technology Co., Ltd.), and subsequently stained with hematoxylin and eosin (H & E) and IHC. Part of the liver metastatic tissues and adjacent normal liver tissue, 0.5 cm away from the tumor tissue, were used for RNA extraction and measurement of mRNA using qPCR. All animal studies were conducted in

accordance with the principles and procedures outlined in the Southern Medical University of China Guide for the Care and Use of Animals.

H & E staining. For H and E staining, 4-μm thick paraffin embedded sections from liver metastatic tissues of nude mice were prepared. The sections were washed in xylene twice for 20 min, then in a descending alcohol series (100% ethanol for 20 min, 100% ethanol for 5 min, 95% alcohol for 5 min, 90% alcohol for 5 min, 80% alcohol for 5 min, 70% alcohol for 5 min) then distilled water for 5 min. The sections were stained with Harris hematoxylin (cat. no. G1004-250; Tiengen Biotech Co., Ltd.) for 3-8 min, and washed with distilled water for 5 min. The sections were subsequently differentiated with 1% hydrochloric acid alcohol for 2 sec then they were washed with distilled water for 5 min, 0.6% ammonia for 5 min, and lastly distilled water for 5 min. The sections were further stained with eosin (cat. no. G1210-2; Tiengen Biotech Co., Ltd.) staining solution for 1-3 min, then washed in an ascending alcohol series (95% alcohol twice for 5 min, 100% ethanol twice for 5 min), and then xylene twice for 5 min. Lastly the sections were air dried and sealed with natural resin All the aforementioned steps were conducted at room temperature.

IHC. Paraffin-embedded sections from liver metastatic tissues of nude mice were cut into 4-μm sections and transferred to glass slides. The slides were deparaffinised with xylene, rehydrated in a descending ethanol series and washed, as aforementioned. The sections were then immersed in 3% hydrogen peroxide to block endogenous peroxidase activity at room temperature for 20 min. The antigen retrieval step were conducted using citrate buffer at 95˚C for 30 min. Non-specific binding was blocked using 5% bovine serum albumin (Sigma-Aldrich; Merck KGaA) at room temperature for 1 h. The sections were subsequently incubated with anti-E-cadherin or anti-vimentin primary antibody at 4˚C overnight then incubated for 1 h at room temperature with a HRP-conjugated goat anti-rabbit IgG (cat. no. PV-6001-6.0) or goat anti-mouse IgG (cat. no. PV-6002-3.0; both OriGene Technologies, Inc.) secondary antibodies. DAB staining solution (cat. no. ZLI-9017; OriGene Technologies, Inc.) was added for 2-8 min and the nuclei were counterstained with hematoxylin for 5 min at room temperature.

Bioinformatics and statistical analysis. The targets of miRNA were predicted using two bioinformatics algorithms: mirwalk2 (http://mirdb.org/miRDB) and TargetScan (http://www.targetscan.org/vert_72). All statistical analyses were performed using SPSS version 22.0 (IBM Corp.). The numerical data with biological replicates are expressed as mean ± standard error. Mann-Whitney U test was used to compare data between two groups. One-way ANOVA was used when comparing the means of multiple groups. Dunnett's post hoc test was used to compare the experimental groups with the control group while Bonferroni's post hoc test was used to compare multiple experimental groups following one-way ANOVA. $P<0.05$ was considered to indicate statistically significant difference. The experimental procedures were performed three times.

Results

miR-500a-5p inhibits EMT in CRC cells. Our previous research demonstrated that miR-500a-5p is a tumor suppressor and inhibits CRC growth (12). To investigate the role of miR-500a-5p in CRC progression, CRC cells were first transfected with miR-500a-5p mimics or inhibitor. As shown in Fig. 1A, miR-500a-5p was significantly upregulated in LoVo-mimics or SW1116-mimics group and downregulated in LoVo-inhibitor or SW1116-inhibitor group compared with that in the negative control (NC) groups.

Second, the function of miR-500a-5p in CRC EMT was investigated. The expression levels of the EMT biomarkers changed in the CRC cell lines following transfection with mimics or with m-NC. The results of the western blot analysis revealed that vimentin expression was markedly reduced in the CRC cells transfected with miR-500a-5p mimics compared with that in cells transfected with m-NC, while E-cadherin expression was notably upregulated. By contrast, the expression of vimentin, was upregulated, whereas that of E-cadherin was downregulated in the CRC cells transfected with miR-500a-5p inhibitor compared with that in cells transfected with i-NC (Fig. 1B).

Studies have shown that oncogenic miRNA promotes tumor cell EMT and metastasis (32,33) and it was found that miR-500a-5p acts as a tumor suppressor in CRC (12). Third, it was determined whether miR-500a-5p inhibitor has any effect on cell EMT. The SW1116 cells transfected with miR-500a-5p inhibitor exhibited decreased E-cadherin expression and increased vimentin expression using immunofluorescence staining under fluorescence microscopy (Fig. 1C).

Fourth, it was observed that the cell structure of LoVo and SW1116 cells transfected with miR-500a-5p inhibitor was transformed from a cubical shape via cellular bonding to a spindle-like shape, and caused spreading of the cells. These changes reflected EMT and were observed via a phase-contrast microscope (Fig. 1D).

Traditionally, actin cytoskeleton transformation is downstream of EMT reprogramming (34). Notably, it is raises questions on how miR-500a-5p can reverse EMT. Finally, the results demonstrated that F-actin filaments formed thick and regular subcortical bundles in LoVo and SW1116 cells transfected miR-500-a-5p inhibitor compared with that in cells transfected with i-NC (Fig. 1E). Therefore, these data indicate that miR-500a-5p inhibits EMT in CRC cells.

TGF-β1-induced EMT is inhibited by miR-500a-5p in CRC cells. TGFβ can activate EMT transcription factors through SMAD-mediated changes in gene expression and signaling pathways that are not mediated by SMADs (17). TGF-β regulates/induces EMT together with other factors (e.g., FGF2 and EGF) (35) and miRNAs regulate TGF-β1-induced EMT in multiple types of cancer. For example, miR-646 attenuates the TGF-b1-induced EMT of gastric cancer cells and miR-141 suppresses EMT in laryngeal cancer through HOXC6-dependent TGF-β signaling pathway (6,36). However, the role of miR-500a-5p in TGF-β1-induced EMT in CRC cells remains unknown. It was found that treatment with TGF-β1 significantly reduced miR-500a-5p expression in a dose/time-dependent manner (Figs. 2A and S1). It was previously demonstrated that

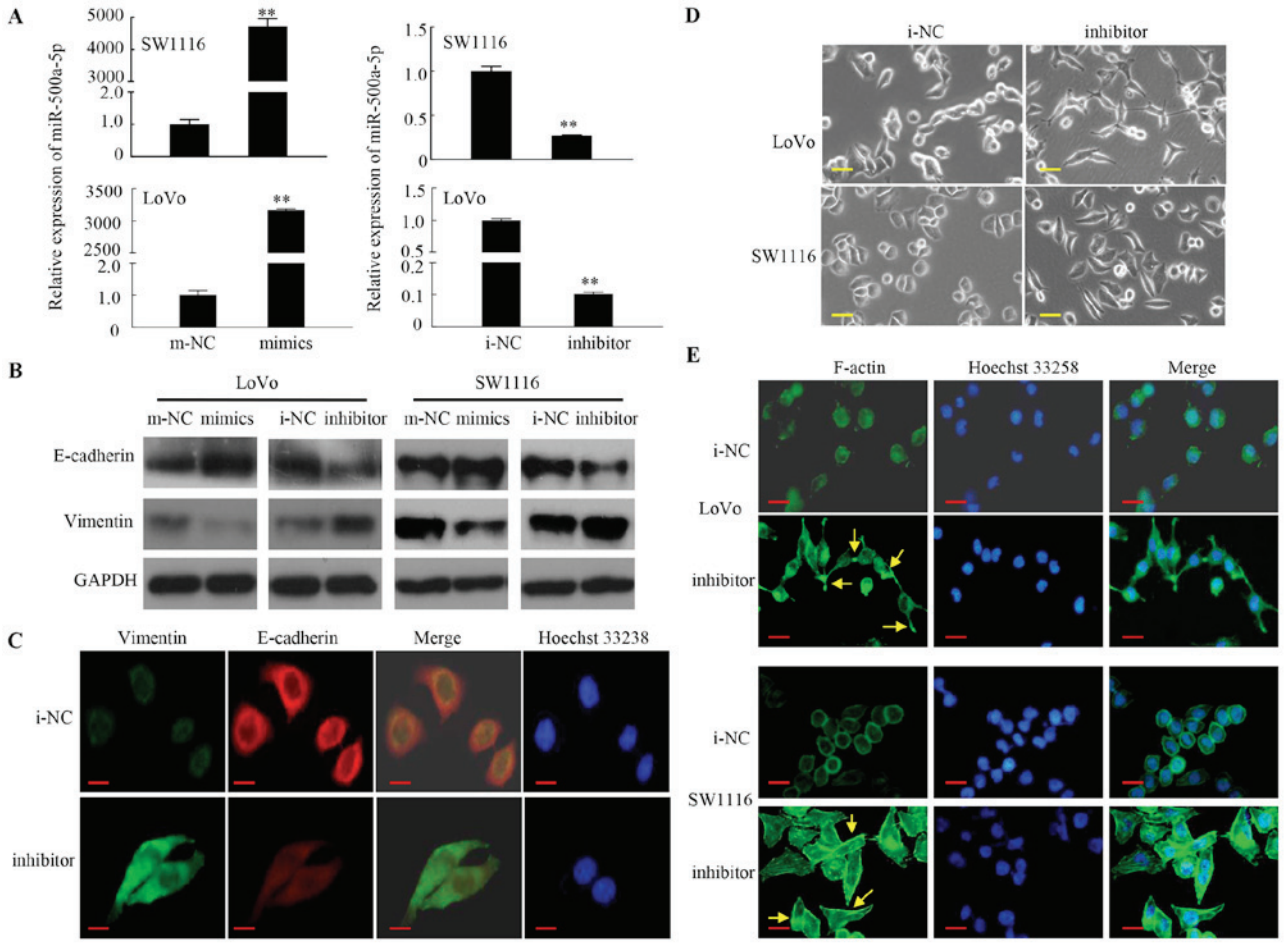

Figure 1. miR-500a-5p suppresses the EMT course in CRC cells. (A) The efficacy of transfection was verified in SW1116 or LoVo cells transfected with miR-500a-5p-mimics and miR-500a-5p-inhibitor. **P<0.05. The data were presented as the mean ± standard error. (B) Protein expression of vimentin and E-cadherin in LoVo and SW1116 using western blot analysis. (C) Immunofluorescent staining of vimentin and E-cadherin in SW1116 cells transfected with miR-500a-5p inhibitor and NC. The scale bars represent 20 μm (D) Cell morphology of CRC cells following transfection with miR-500a-5p-inhibitor and NC. The scale bars represent 50 μm. (E) The F-actin cytoskeletal arrangement was examined using fluorescence microscopy following transfection of CRC cells with miR-500a-5p inhibitor and NC. The scale bars represent 50 μm. miR, microRNA; EMT, epithelia-mesenchymal transition; CRC, colorectal cancer; NC, negative control; m, mimic; i, inhibitor.

CRC cells exhibited a myofibroblast-like phenotype caused by TGF-β1 (34). As shown in Fig. 2B, enhancing miR-500a-5p expression suppressed the transformation of CRC cells to a myofibroblast structure when treated with TGF-β1. Moreover, increased miR-500a-5p expression was associated with a markedly decrease in the protein levels of vimentin and an increase in the protein levels of E-cadherin when compared with that in the TGF-β1 group (Fig. 2C). The green signals denote Vimentin staining, while the red signals denote E-cadherin staining using immunofluorescence staining under a fluorescence microscopy. The results revealed that TGF-β1 treatment decreased the expression of E-cadherin and increased the expression of vimentin; while miR-500a-5p overexpression reversed the TGF-β1-mediated upregulation of vimentin and downregulation of E-cadherin (Fig. 2D). Furthermore, the Transwell experiments demonstrated that upregulated miR-500a-5p expression inhibited the effects of TGF-β1 on tumor cell invasion ability (Fig. 2E). The results suggest that miR-500a-5p reduces TGF-β1-induced EMT in CRC cells.

miR-500a-5p inhibitor-induced EMT is suppressed by emodin in CRC cells. It was previously reported that emodin inhibits RKO CRC cell invasion and migration by suppressing EMT (37). A total of three CRC cell lines at Dukes' stage A (SW1116), B (SW480) and C (LoVo) were selected from the American Type Culture Collection to investigate whether the effect of emodin is independent of the progression status in cells undergoing EMT. The western blot analysis indicated that increasing emodin concentrations markedly decreased the mesenchymal marker expression, vimentin, but increased the epithelial marker, E-cadherin, levels in SW1116, SW480 and LoVo cells (Fig. 3A).

To highlight the emodin regulation of miR-500a-5p in EMT during CRC cell metastasis, the EMT marker levels were investigated. The protein expression level of E-cadherin was significantly decreased, and expression level of vimentin was increased by miR-500a-5p inhibitor, whereas emodin treatment partially reversed EMT compared with that in i-NC CRC cells (Fig. 3B).

Furthermore, miR-500a-5p inhibitor promoted EMT and lead to mesenchymal changes in CRC cells, which resulted in a long fusiform shape, whereas cells treated with emodin and miR-500-a-5p inhibitor did not exhibit scattering as seen in cells transfected with miR-500a-5p inhibitor only (Fig. 3C).

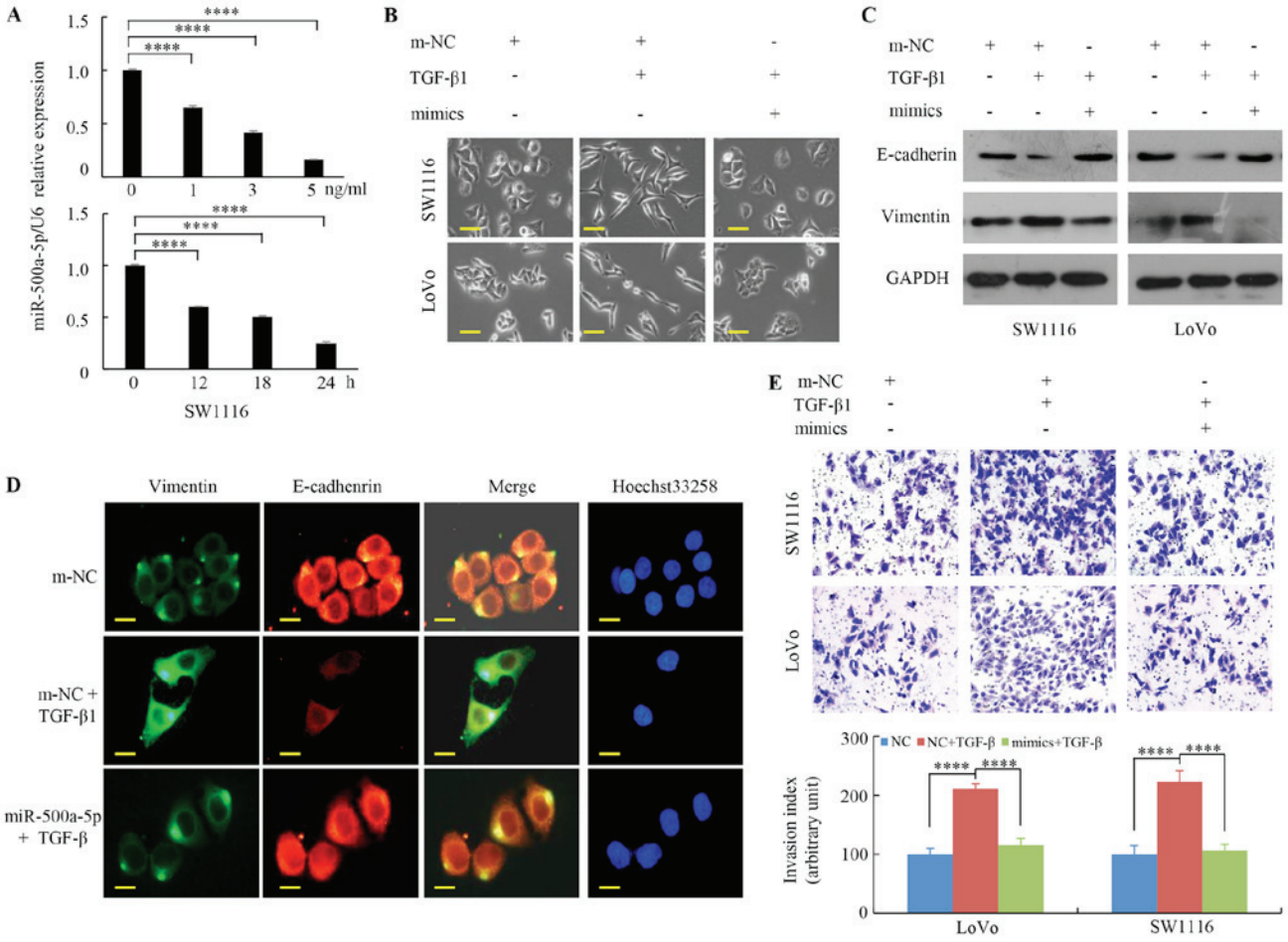

Figure 2. miR-500a-5p attenuates TGF-β1-induced EMT in CRC cells. (A) miR-500a-5p expression was dose- and time-dependently decreased following treatment with TGF-β1 in SW1116 cells detected using reverse transcription-quantitative PCR. The data are presented as the mean ± standard error from 3 independent experiments. ****P<0.001. (B) Cell morphology of CRC cells following transfection with miR-500a-5p-mimics or NC and treatment with TGF-β1 for 24 h and were visualized using phase-contrast microscopy. The scale bars represent 50 μm. (C) Western blot analysis of vimentin and E-cadherin protein expression revealed that miR-500a-5p mimic inhibited EMT in CRC cells following treatment with TGF-β1. (D) EMT biomarker protein expression levels in CRC cells transfected with miR-500a-5p mimic or NC and treated with TGF-β1 measured using immunofluorescent assays. The scale bars represent 20 μm. (E) Representaive images from Matrigel assay following transfection of miR-500a-5p mimic or NC and treatment with TGF-β1, and quantified results. ****P<0.001. miR, microRNA; EMT, epithelia-mesenchymal transition; CRC, colorectal cancer; NC, negative control; m, mimic; i, inhibitor; TGF-β, transforming growth factor-β.

In addition, in the miR-500a-5p inhibitor group, F-actin was distributed along the long axis of the cells, which is a hallmark of the mesenchymal phenotype. However, treatment of the miR-500a-5p inhibitor-transfected cells with emodin caused mesenchymal-to-epithelial transition, which is the opposite of EMT (Fig. 3D).

Lastly, it was observed that cells transfected with miR-500a-5p inhibitor significantly increased the numbers of invading cells, whereas the activating effect of the miR-500a-5p inhibitor on CRC cell invasion was abolished by emodin (Fig. 3E). This result indicates that emodin suppresses miR-500a-5p inhibitor-induced EMT in CRC cells.

miR-500a-5p affects tumor metastasis by regulating EMT in CRC cells in vivo. To investigate the association between miR-500a-5p and tumor metastasis via EMT regulation, miR-500a-5p/LoVo cells and m-NC/LoVo cells, with RFP expression, were established to visualise tumor metastasis. A total of one month following orthotopic spleen injections in nude mice, the animals were euthanised and their livers were examined. The number of tumor metastatic liver nodules in the miR-500a-5p/LoVo mouse group was significantly lower compared with that in the m-NC/LoVo group (Fig. 4A and B). The corresponding HE and IHC images of the liver are shown in Fig. 4C and D, respectively. Brown-yellow signals indicate vimentin or E-cadherin staining. The protein expression level of E-cadherin was downregulated, while that of vimentin was upregulated in liver cancer tissues compared with that in adjacent normal liver tissues in miR-500a-5p mimic group (Fig. 4D).

Moreover, the orthotopic implantation of miR-500a-5p/LoVo cells led to increased E-cadherin, and decreased vimentin mRNA expression levels in liver cancer tissues, compared with that in the mice implanted with m-NC (Fig. 4E). These results indicate that miR-500a-5p affects tumor metastasis by regulating EMT in CRC cells *in vivo*.

Discussion

Previous research suggests that miRNAs modulate tumor-associated gene expression and affect cancer progression (38-41). For example, miR-300 inhibits cell invasion and regulates EMT-related marker genes by targeting TWIST in head and

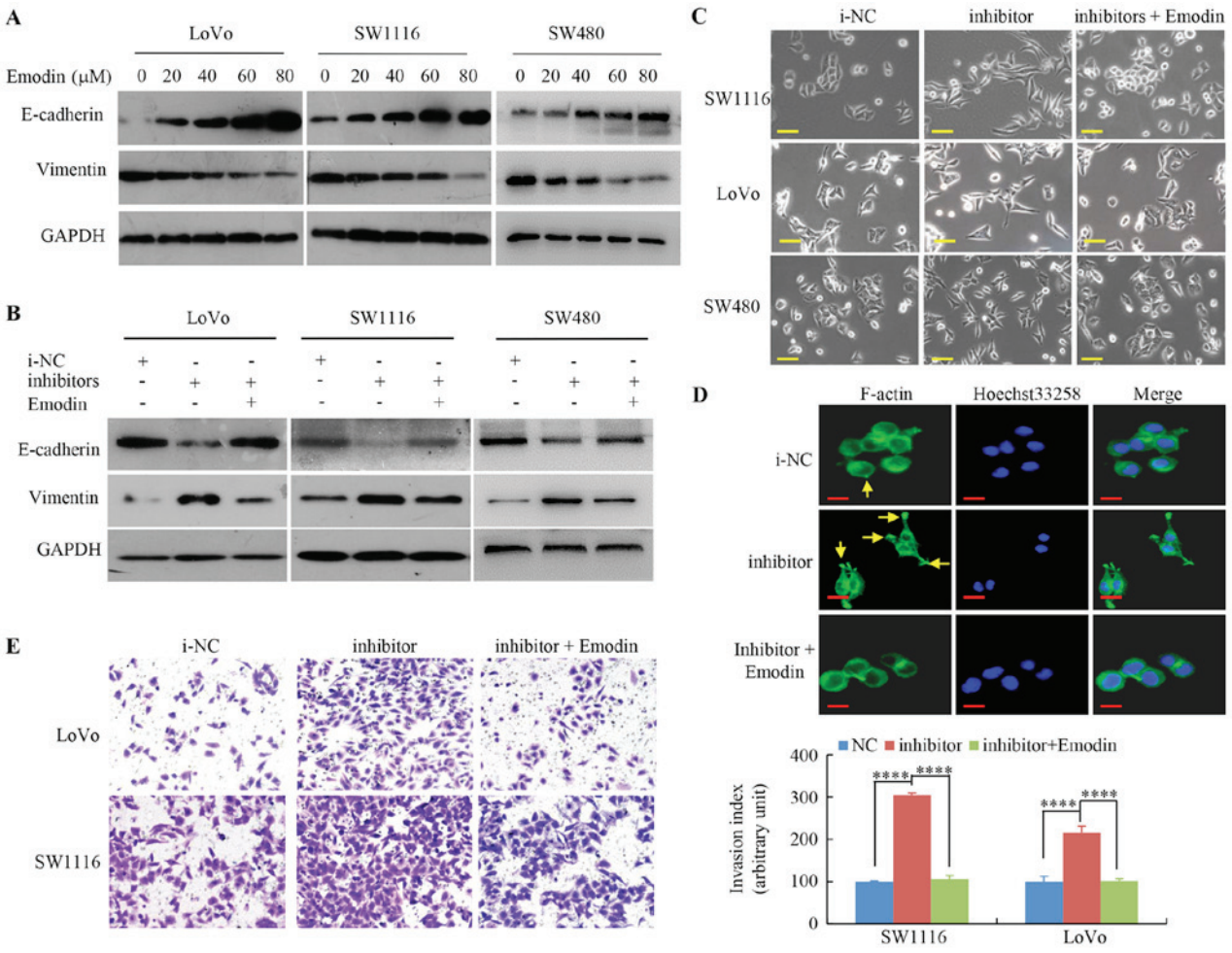

Figure 3. miR-500a-5p-induced EMT is suppressed by emodin in CRC cells. (A) CRC cells were treated with different concentrations of emodin for 2 days, and the vimentin and E-cadherin protein expression levels were examined using western blot analysis. (B) E-cadherin and vimentin protein expression levels were detected using western blot analysis in CRC cells transfected with miR-500a-5p inhibitor or NC, following treatment with emodin. (C) Cell morphology and (D) F-actin cytoskeletal arrangement of CRC cells transfected with miR-500a-5p inhibitor or NC and/or treated with emodin. Scale bars represent 50 μm in (C) and 20 μm in (D). (E) Matrigel assay was used determine the invasive potential of CRC cells transfected with miR-500a-5p inhibitor or NC following treatment with emodin. Data are presented as the mean ± standard error. ****P<0.001. miR, microRNA; EMT, epithelia-mesenchymal transition; CRC, colorectal cancer; NC, negative control; m, mimic; i, inhibitor.

neck squamous cell carcinoma (39). Moreover, overexpression of miR-300, using miR-330 mimics, suppressed cell invasion *in vitro* and experimental metastasis *in vivo* (39). Several previous studies have also reported the role of miR-500a-5p in the development of the malignant tumor, in liver cancer (8), chronic lymphocytic leukemia (9) and breast cancer (10). However, research on the function of miR-500a-5p in CRC development in the literature is limited. In the present study, miR-500a-5p was found to inhibit the metastasis and EMT in CRC cells. Moreover, increased miR-500a-5p expression attenuated TGF-b1-induced EMT. In addition, miR-500a-5p inhibitor-induced EMT was suppressed by emodin. These findings suggest that miR-500a-5p affects CRC progression and may be beneficial as a therapeutic target.

EMT occurs during embryonic stage, healing of lesions and cancer progression (13,15,42,43). During EMT, cytoskeletal restructuring occurs, resulting in loss of polarity and mesenchymal phenotype changes, loss of cellular junctions and increased migratory potential. miRNAs may act as tumor suppressors or oncogenes (5,6,33,36,39). It has been suggested that some miRNAs regulate EMT during cancer progression and metastasis. For example, Liu *et al* (19) confirmed that miR-1271 modulates EMT in pancreatic cancer cells metastasis by targeting ZEB1 and TWIST1, increasing E-cadherin and decreasing vimentin protein expression levels. In the present study it was revealed that miR-500a-5p is involved in CRC metastasis through EMT regulation. It was demonstrated that miR-500a-5p inhibitor induces EMT and the metastatic phenotype. The results were consistent with the outcomes of a previous investigation, which revealed that overexpression of miR-708 inhibits motility, migration and invasion of CRC cells and suppresses EMT (44). The results of the present study indicate that miR-500a-5p plays a role in EMT of CRC cells, and this may be one of the factors affecting the development of CRC. In addition, miRNAs play key roles by regulating target gene expression. Therefore, two algorithms that predict the mRNA targets of a miRNA were used. Zinc finger E-box binding homeobox ZEB1 and ZEB2 were identified as potential target genes of miR-500a-5p in cancer cells, including CRC cells using bioinformatics analysis. ZEB family is known as a transcription factor, whose family members include ZEB1 and ZEB2, which are important factors for EMT (45). However,

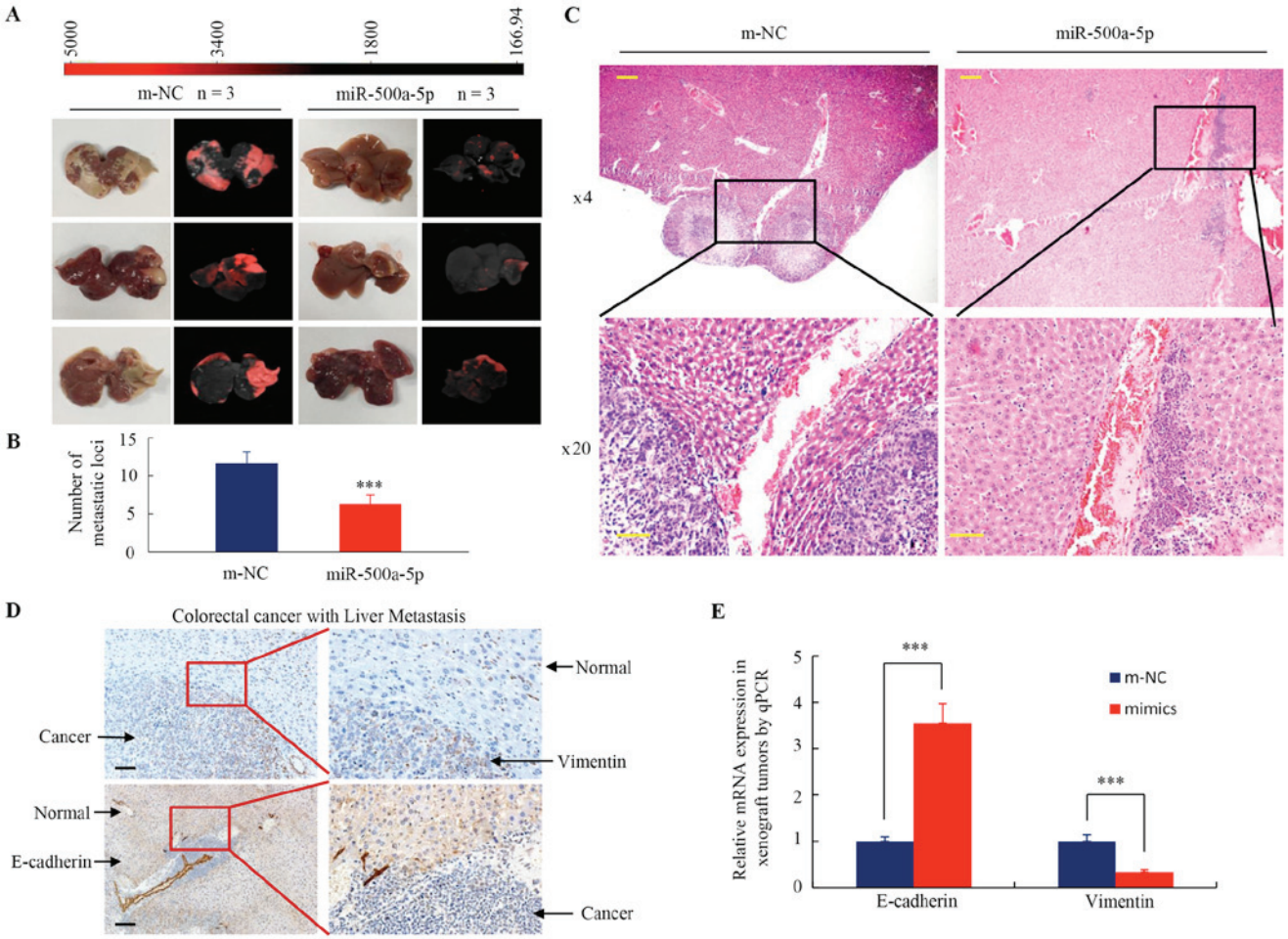

Figure 4. miR-500a-5p modulates EMT and CRC metastasis. (A) Nude mice underwent orthotopic spleen injections with LoVo/miR-500a-5p cells or LoVo/m-NC cells. The red fluorescent protein of liver metastatic lesions were examined using an *In Vivo* F Imaging System. (B) The number of liver micro-metastasis foci was measured. ***P<0.01. (C) Hemotoxylin and eosin was used to stain the tumor cell metastatic tissues. (D) Gene expression was determined in CRC cell-derived liver metastases using immunohistochemistry. (E) Gene expression in tumors extracted from LoVo cells was determined using reverse transcription-quantitative PCR. ***P<0.01. Scale bars represent 200 μm in (C) and (D).

further studies are required to elucidate how miR-500a-5p modulates ZEB1 and/or ZEB2 to promote EMT in CRC cells.

Rearrangement of the actin cytoskeleton is the major mechanism driving cell migration and invasion during the process of EMT, and promoting invasive behaviour of cancer cells (46,47). Previous studies indicated that miRNAs modulate actin cytoskeleton organization in cancer cells. For example, Liu *et al* (48) revealed that miR-144-3p significantly inhibited proliferation, migration and invasion in GC cells. Moreover, overexpression of miR-144-3p by its mimics disrupted the cytoskeleton of GC cells by decreasing f-actin expression, thus may affect GC metastasis and invasion by regulating EMT. Jurmeister *et al* (49) reported that miR-200c also inhibits breast cancer cell migration via the same cytoskeletal reorganization, which markedly reduces the formation of lamellipodia, and reverses EMT. This is consistent with the results from the present study as it was found that the miR-500a-5p inhibitor promoted rearrangements in the actin cytoskeleton and resulted in an increase of F-actin microfilaments. Thus, it was demonstrated that cytoskeletal organization was also regulated by miR-500a-5p in CRC cells.

TGF-β signaling can suppress or promote the development of tumors, which may vary according to cancer stage (14,18,50). TGF-β signaling prevents tumor progression by initiating programmed cell death, particularly during the early stages of cancer, including CRC (50). However, TGF-β signaling promotes EMT-mediated cancer cell invasion and metastasis in the later stages. For example, upregulated TGF-β can induce EMT through Smad2 and Smad3 activation, thus, promoting cancer cell invasion and metastasis to the progressive stage (51). Numerous studies have reported the involvement of miRNAs in TGF-β-induced EMT (5,6,36). For example, Chen *et al* (36) demonstrated that upregulation of miR-141 suppresses EMT and lymph node metastasis in laryngeal cancer through suppressing HOXC6-dependent TGF-β signaling pathway. In the present study, miR-500a-5p expression decreased in a dose and time-dependent manner in the CRC cells treated with TGF-β. miR-500a-5p reversed the EMT phenotype of CRC cells. Moreover, incubation of cells transfected with miR-500a-5p decreased TGF-β-mediated cell invasion, which was similar to the effect of miR-630 on hepatocellular carcinoma cells (52). The findings from the present study strongly suggest that miR-500a-5p may be a downstream inhibitor of the TGF-β signaling pathway, reducing the effects of TGF-β on CRC cells.

Emodin exerts a direct inhibitory effect on the growth and metastasis of a variety of malignant tumor cells. For example, emodin causes inhibition of growth of K562 leukaemia cells

and improves survival (53). Emodin inhibits CRC cell invasion and migration (37) and also inhibits EMT (54), as demonstrated by increased E-cadherin and decreased fibronectin, a-smooth muscle actin, N-cadherin and vimentin protein expression levels, together with reduced expression of the transcriptional repressors Slug, Twist and Snail. Multiple previous studies have demonstrated that treatment with emodin inhibits the EMT process and metastasis by regulating miRNAs (28,29). For example, emodin inhibits pancreatic cancer EMT and invasion by upregulating miR-1271 (29). The results from the present study are consistent with previous studies, which indicates that the miR-500a-5p inhibitor initiates EMT in CRC cells, whereas emodin can prevent this process. Treatment with emodin blocked miR-500a-5p inhibitor-initiated cell invasion and caused alterations in cellular morphology. Moreover, emodin inhibited miR-500a-5p inhibitor-induced cell invasion. Thus, emodin suppressed miR-500a-5p inhibitor-induced EMT, thereby exerting therapeutic and preventive effects by suppressing the metastasis of CRC cells.

In conclusion, EMT and CRC cell invasion are inhibited by miR-500a-5p. In addition, overexpression of miR-500a-5p attenuates TGF-β1-induced EMT, whereas emodin suppresses miR-500a-5p inhibitor-induced EMT in CRC cells. These results uncovered the EMT-suppressive role of miR-500a-5p, which may be used for the development of novel therapeutic strategies for CRC.

Acknowledgements

Not applicable.

Funding

This project was funded by the National Natural Science Funds of China (grant nos. 81672875, 81772964 and 81974448); Guangdong Gastrointestinal Disease Research Center (grant no. 2017B02029003); Special Scientific Research Fund of Public Welfare Profession of National Health and Family Planning Commission (grant no. 201502026); Guangdong Medical Science and Technology Research Foundation (grant no. B2019126); Science and technology innovation foundation of Shenzhen (grant no. JCYJ20180306170328854).

Availability of data and materials

The datasets generated and/or analyzed during the current study are available from the corresponding author upon reasonable request.

Authors' contributions

WT and WD performed the *in vitro* experiments. JLi, HZ, JLin and YW contributed to acquisition, analysis and interpretation of the data. QY, ML and YX performed the *in vivo* experiments. ZL, YZ, XW and JinW revised the manuscript critically for important intellectual content. YC, HH and SL made substantial contributions to conception and design of the study. JidW and LX drafted the manuscript. LH revised the manuscript. The final manuscript for publication was read and approved by all authors.

Ethics approval and consent to participate

The study was ethically approved by Southern Medical University Experimental Animal Ethics Committee.

Patient consent for publication

Not applicable.

Competing interests

The authors declare that they have no competing interests.

References

1. Finlay IG and McArdle CS: Effect of occult hepatic metastases on survival after curative resection for colorectal carcinoma. Gastroenterology 85: 596-599, 1983.
2. Kemp Z, Thirlwell C, Sieber O, Silver A and Tomlinson I: An update on the genetics of colorectal cancer. Hum Mol Genet 13 Spec No 2: R177-185, 2004.
3. Konishi M, Kikuchi-Yanoshita R, Tanaka K, Muraoka M, Onda A, Okumura Y, Kishi N, Iwama T, Mori T, Koike M, *et al*: Molecular nature of colon tumors in hereditary nonpolyposis colon cancer, familial polyposis, and sporadic colon cancer. Gastroenterology 111: 307-317, 1996.
4. van Erning FN, Crolla RM, Rutten HJ, Beerepoot LV, van Krieken JH and Lemmens VE: No change in lymph node positivity rate despite increased lymph node yield and improved survival in colon cancer. Eur J Cancer 50: 3221-3229, 2014.
5. Zhang F, Luo Y, Shao Z, Xu L, Liu X, Niu Y, Shi J, Sun X, Liu Y, Ding Y and Zhao L: MicroRNA-187, a downstream effector of TGFβ pathway, suppresses Smad-mediated epithelial-mesenchymal transition in colorectal cancer. Cancer Lett 373: 203-213, 2016.
6. Zhang P, Tang WM, Zhang H, Li YQ, Peng Y, Wang J, Liu GN, Huang XT, Zhao JJ, Li G, *et al*: MiR-646 inhibited cell proliferation and EMT-induced metastasis by targeting FOXK1 in gastric cancer. Br J Cancer 117: 525-534, 2017.
7. Liu X, Li J, Yu Z, Li J, Sun R and Kan Q: miR-935 promotes liver cancer cell proliferation and migration by targeting SOX7. Onco Res 25: 427-435, 2017.
8. Guo Y, Chen L, Sun C and Yu C: MicroRNA-500a promotes migration and invasion in hepatocellular carcinoma by activating the Wnt/β-catenin signaling pathway. Biomed Pharmacother 91: 13-20, 2017.
9. Ruiz-Lafuente N, Alcaraz-Garcia MJ, Sebastian-Ruiz S, Garcia-Serna AM, Gomez-Espuch J, Moraleda JM, Minguela A, Garcia-Alonso AM and Parrado A: IL-4 Up-regulates MiR-21 and the MiRNAs hosted in the CLCN5 gene in chronic lymphocytic leukemia. PLoS One 10: e0124936, 2015.
10. Degli Esposti D, Aushev VN, Lee E, Cros MP, Zhu J, Herceg Z, Chen J and Hernandez-Vargas H: miR-500a-5p regulates oxidative stress response genes in breast cancer and predicts cancer survival. Sci Rep 7: 15966, 2017.
11. Jiang M, Zhou LY, Xu N and An Q: Down-regulation of miR-500 and miR-628 suppress non-small cell lung cancer proliferation, migration and invasion by targeting ING1. Biomed Pharmacother 108: 1628-1639, 2018.
12. Tang W, Zhou W, Xiang L, Wu X, Zhang P, Wang J, Liu G, Zhang W, Peng Y, Huang X, *et al*: The p300/YY1/miR-500a-5p/HDAC2 signalling axis regulates cell proliferation in human colorectal cancer. Nat Commun 10: 663, 2019.
13. Yang MH, Wu MZ, Chiou SH, Chen PM, Chang SY, Liu CJ, Teng SC and Wu KJ: Direct regulation of TWIST by HIF-1alpha promotes metastasis. Nat Cell Biol 10: 295-305, 2008.
14. Zhang W, Jiang B, Guo Z, Sardet C, Zou B, Lam CS, Li J, He M, Lan HY, Pang R, *et al*: Four-and-a-half LIM protein 2 promotes invasive potential and epithelial-mesenchymal transition in colon cancer. Carcinogenesis 31: 1220-1229, 2010.
15. Yan Q, Zhang W, Wu Y, Wu M, Zhang M, Shi X, Zhao J, Nan Q, Chen Y, Wang L, *et al*: KLF8 promotes tumorigenesis, invasion and metastasis of colorectal cancer cells by transcriptional activation of FHL2. Oncotarget 6: 25402-25417, 2015.

16. Huang X, Xiang L, Li Y, Zhao Y, Zhu H, Xiao Y, Liu M, Wu X, Wang Z, Jiang P, *et al*: Snail/FOXK1/Cyr61 signaling axis regulates the epithelial-mesenchymal transition and metastasis in colorectal cancer. Cell Physiol Biochem 47: 590-603, 2018.
17. Lamouille S, Xu J and Derynck R: Molecular mechanisms of epithelial-mesenchymal transition. Nature reviews. Mol Cell Biol 15: 178-196, 2014.
18. Fan Y, Shen B, Tan M, Mu X, Qin Y, Zhang F and Liu Y: TGF-β-induced upregulation of malat1 promotes bladder cancer metastasis by associating with suz12. Clin Cancer Res 20: 1531-1541, 2014.
19. Liu H, Wang H, Liu X and Yu T: miR-1271 inhibits migration, invasion and epithelial-mesenchymal transition by targeting ZEB1 and TWIST1 in pancreatic cancer cells. Biochem Biophys Res Commun 472: 346-352, 2016.
20. Demirezer LO, Kuruuzum-Uz A, Bergere I, Schiewe HJ and Zeeck A: The structures of antioxidant and cytotoxic agents from natural source: Anthraquinones and tannins from roots of Rumex patientia. Phytochemistry 58: 1213-1217, 2001.
21. Huang Q, Lu G, Shen HM, Chung MC and Ong CN: Anti-cancer properties of anthraquinones from rhubarb. Med Res Rev 27: 609-630, 2007.
22. Li J, Liu P, Mao H, Wanga A and Zhang X: Emodin sensitizes paclitaxel-resistant human ovarian cancer cells to paclitaxel-induced apoptosis in vitro. Oncol Rep 21: 1605-1610, 2009.
23. Dong X, Fu J, Yin X, Cao S, Li X, Lin L; Huyiligeqi and Ni J: Emodin: A review of its pharmacology, toxicity and pharmacokinetics. Phytother Res 30: 1207-1218, 2016.
24. Ko JC, Su YJ, Lin ST, Jhan JY, Ciou SC, Cheng CM and Lin YW: Suppression of ERCC1 and Rad51 expression through ERK1/2 inactivation is essential in emodin-mediated cytotoxicity in human non-small cell lung cancer cells. Biochem Pharmacol 79: 655-664, 2010.
25. He Y, Huang J, Wang P, Shen X, Li S, Yang L, Liu W, Suksamrarn A, Zhang G and Wang F: Emodin potentiates the antiproliferative effect of interferon α/β by activation of JAK/STAT pathway signaling through inhibition of the 26S proteasome. Oncotarget 7: 4664-4679, 2016.
26. Cai J, Niu X, Chen Y, Hu Q, Shi G, Wu H, Wang J and Yi J: Emodin-induced generation of reactive oxygen species inhibits RhoA activation to sensitize gastric carcinoma cells to anoikis. Neoplasia 10: 41-51, 2008.
27. van Gorkom BA, Timmer-Bosscha H, de Jong S, van der Kolk DM, Kleibeuker JH and de Vries EG: Cytotoxicity of rhein, the active metabolite of sennoside laxatives, is reduced by multidrug resistance-associated protein 1. Br J Cancer 86: 1494-1500, 2002.
28. Niu Y, Zhang J, Tong Y, Li J and Liu B: Physcion 8-O-β-glucopyranoside induced ferroptosis via regulating miR-103a-3p/GLS2 axis in gastric cancer. Life Sci 237: 116893, 2019.
29. Li N, Wang C, Zhang P and You S: Emodin inhibits pancreatic cancer EMT and invasion by upregulating microRNA1271. Mol Med Rep 18: 3366-3374, 2018.
30. Wang J, Yang Y, Xia HH, Gu Q, Lin MC, Jiang B, Peng Y, Li G, An X, Zhang Y, *et al*: Suppression of FHL2 expression induces cell differentiation and inhibits gastric and colon carcinogenesis. Gastroenterology 132: 1066-1076, 2007.
31. Livak KJ and Schmittgen TD: Analysis of relative gene expression data using real-time quantitative PCR and the 2(-Delta Delta C(T)) method. Methods 25: 402-408, 2001.
32. Liu B, Li X, Li C, Xu R and Sun X: miR-25 mediates metastasis and epithelial-mesenchymal-transition in human esophageal squamous cell carcinoma via regulation of E-cadherin signaling. Bioengineered 10: 679-688, 2019.
33. Li S, Hou X, Wu C, Han L, Li Q, Wang J and Luo S: MiR-645 promotes invasiveness, metastasis and tumor growth in colorectal cancer by targeting EFNA5. Biomed Pharmacother 125: 109889, 2020.
34. Huang HC, Hu CH, Tang MC, Wang WS, Chen PM and Su Y: Thymosin beta4 triggers an epithelial-mesenchymal transition in colorectal carcinoma by upregulating integrin-linked kinase. Oncogene 26: 2781-2790, 2007.
35. Schelch K, Wagner C, Hager S, Pirker C, Siess K, Lang E, Lin R, Kirschner MB, Mohr T, Brcic L, *et al*: FGF2 and EGF induce epithelial-mesenchymal transition in malignant pleural mesothelioma cells via a MAPKinase/MMP1 signal. Carcinogenesis 39: 534-545, 2018.
36. Chen L, Sun DZ, Fu YG, Yang PZ, Lv HQ, Gao Y and Zhang XY: Upregulation of microRNA-141 suppresses epithelial-mesenchymal transition and lymph node metastasis in laryngeal cancer through HOXC6-dependent TGF-β signaling pathway. Cell Signal 66: 109444, 2020.
37. Gu J, Cui CF, Yang L, Wang L and Jiang XH: Emodin inhibits colon cancer cell invasion and migration by suppressing epithelial-mesenchymal transition via the Wnt/β-catenin pathway. Oncol Res 27: 193-202, 2019.
38. Larsson O, Li S, Issaenko OA, Avdulov S, Peterson M, Smith K, Bitterman PB and Polunovsky VA: Eukaryotic translation initiation factor 4E induced progression of primary human mammary epithelial cells along the cancer pathway is associated with targeted translational deregulation of oncogenic drivers and inhibitors. Cancer Res 67: 6814-6824, 2007.
39. Yu J, Xie F, Bao X, Chen W and Xu Q: miR-300 inhibits epithelial to mesenchymal transition and metastasis by targeting Twist in human epithelial cancer. Mol Cancer 13: 121, 2014.
40. Akao Y, Nakagawa Y, Hirata I, Iio A, Itoh T, Kojima K, Nakashima R, Kitade Y and Naoe T: Role of anti-oncomirs miR-143 and -145 in human colorectal tumors. Cancer Gene Ther 17: 398-408, 2010.
41. Liu F, Cai Y, Rong X, Chen J, Zheng D, Chen L, Zhang J, Luo R, Zhao P and Ruan J: MiR-661 promotes tumor invasion and metastasis by directly inhibiting RB1 in non small cell lung cancer. Mol Cancer 16: 122, 2017.
42. Huang C, Xie D, Cui J, Li Q, Gao Y and Xie K: FOXM1c promotes pancreatic cancer epithelial-to-mesenchymal transition and metastasis via upregulation of expression of the urokinase plasminogen activator system. Clin Cancer Res 20: 1477-1488, 2014.
43. Qi H, Fu X, Li Y, Pang X, Chen S, Zhu X, Li F and Tan W: SATB1 promotes epithelial-mesenchymal transition and metastasis in prostate cancer. Oncol Lett 13: 2577-2582, 2017.
44. Sun S, Hang T, Zhang B, Zhu L, Wu Y, Lv X, Huang Q and Yao H: miRNA-708 functions as a tumor suppressor in colorectal cancer by targeting ZEB1 through Akt/mTOR signaling pathway. Am J Transl Res 11: 5338-5356, 2019.
45. Guan T, Dominguez CX, Amezquita RA, Laidlaw BJ, Cheng J, Henao-Mejia J, Williams A, Flavell RA, Lu J and Kaech SM: ZEB1, ZEB2, and the miR-200 family form a counterregulatory network to regulate $CD8^+$ T cell fates. J Exp Med 215: 1153-1168, 2018.
46. Sousa-Squiavinato ACM, Rocha MR, Barcellos-de-Souza P, de Souza WF and Morgado-Diaz JA: Cofilin-1 signaling mediates epithelial-mesenchymal transition by promoting actin cytoskeleton reorganization and cell-cell adhesion regulation in colorectal cancer cells. Biochim Biophys Acta Mol Cell Res 1866: 418-429, 2019.
47. Islam SU, Ahmed MB, Lee SJ, Shehzad A, Sonn JK, Kwon OS and Lee YS: PRP4 kinase induces actin rearrangement and epithelial-mesenchymal transition through modulation of the actin-binding protein cofilin. Exp Cell Res 369: 158-165, 2018.
48. Liu F, Chen N, Xiao R, Wang W and Pan Z: miR-144-3p serves as a tumor suppressor for renal cell carcinoma and inhibits its invasion and metastasis by targeting MAP3K8. Biochem Biophys Res Commun 480: 87-93, 2016.
49. Jurmeister S, Baumann M, Balwierz A, Keklikoglou I, Ward A, Uhlmann S, Zhang JD, Wiemann S and Sahin O: MicroRNA-200c represses migration and invasion of breast cancer cells by targeting actin-regulatory proteins FHOD1 and PPM1F. Mol Cell Biol 32: 633-651, 2012.
50. Shen W, Tao GQ, Zhang Y, Cai B, Sun J and Tian ZQ: TGF-β in pancreatic cancer initiation and progression: Two sides of the same coin. Cell Biosci 7: 39, 2017.
51. Zhou Q, Zheng X, Chen L, Xu B, Yang X, Jiang J and Wu C: Smad2/3/4 pathway contributes to TGF-β-Induced MiRNA-181b expression to promote gastric cancer metastasis by targeting Timp3. Cell Physiol Biochem 39: 453-466, 2016.
52. Chen WX, Zhang ZG, Ding ZY, Liang HF, Song J, Tan XL, Wu JJ, Li GZ, Zeng Z, Zhang BX and Chen XP: MicroRNA-630 suppresses tumor metastasis through the TGF-beta- miR-630-Slug signaling pathway and correlates inversely with poor prognosis in hepatocellular carcinoma. Oncotarget 7: 22674-22686, 2016.
53. Chun-Guang W, Jun-Qing Y, Bei-Zhong L, Dan-Ting J, Chong W, Liang Z, Dan Z and Yan W: Anti-tumor activity of emodin against human chronic myelocytic leukemia K562 cell lines in vitro and in vivo. Eur J Pharmacol 627: 33-41, 2010.
54. Han YT, Chen XH, Gao H, Ye JL and Wang CB: Physcion inhibits the metastatic potential of human colorectal cancer SW620 cells in vitro by suppressing the transcription factor SOX2. Acta Pharmacol Sin 37: 264-275, 2016.